

Bremsstrahlung Cross-Section Measurements at Incident Electron Energies of 1.0, 1.7, and 2.5 MeV*

D. H. RESTER AND W. E. DANCE

LTV Research Center, Ling-Temco-Vought, Incorporated, Dallas, Texas

(Received 3 April 1967)

Measurements of electron-bremsstrahlung cross sections have been made for incident electron energies of 1.0, 1.7, and 2.5 MeV and targets of Al, Cu, Sn, and Au. Data are included at angles of observation from 0° to a limiting angle including more than 90% of the total emitted bremsstrahlung at each incident electron energy. The present measurements are lower than the results of Motz for Al and Au at 1.0 MeV; however, the present results at 2.5 MeV agree with the results of Starfelt and Koch at 2.72 MeV. Comparison with the Born approximation indicates that the experimental cross sections are larger than predicted near the high-frequency limit. This effect increases with atomic number at a given energy but decreases with energy, as expected.

INTRODUCTION

A REVIEW of the electron-bremsstrahlung process was published in 1959 by Koch and Motz.¹ This review paper gives a summary of the bremsstrahlung cross-section formulas and the related experimental data. In the intermediate energy region, i.e., from 0.1 to 3.0 MeV, the cross-section formulas available for comparison with experiment are calculated by the Born-approximation procedure with free-particle wave functions. Only at low incident electron energy does an exact bremsstrahlung theory exist. The Born-approximation theory is known to yield less accurate results as (1) the incident electron energy decreases, (2) the atomic number of the scattering atom increases, and (3) the photon energy approaches the incident electron energy. It is therefore expected that in the intermediate energy region the theoretical predictions presently available will give only reasonably good results. Experiments at the time of the review article in this energy region confirm this conclusion. The data of Motz² at 0.5- and 1.0-MeV incident electron energies are generally higher than the Born-approximation theory. Discrepancies of as much as a factor of 3 between the experimental and theoretical values were observed for Au ($Z=79$) targets at photon energies h near the mid-energy points of the spectra for angles of 60° and 90° and for an incident electron energy $T_0=0.5$ MeV. Even at 1.0 MeV for Be ($Z=4$) and Al ($Z=13$) targets, the experimental values at 10° average 75% higher than the Born-approximation values. On the other hand, at $T_0=2.72$ MeV, [Starfelt and Koch³ measured cross-section values at 0° for both Al and Au targets which are below the Born-approximation values for all photon energies. At 6.03° their reported values in the photon energy region $h>400$ keV are in good agreement with the theory and are below the theory for $h<400$ keV.

To bridge the gap in the experimental results from the 1.0-MeV data of Motz to the 2.72-MeV data of Starfelt and Koch, the present systematic experimental study was undertaken. It includes measurements of electron-bremsstrahlung cross sections for incident electron energies of 1.0, 1.7, and 2.5 MeV for targets of Al, Cu, Sn, and Au. A NaI(Tl) scintillation spectrometer was used to obtain the bremsstrahlung spectral distributions. The electron beam was provided by a Van de Graaff accelerator. Angles at which cross sections were measured varied with the incident energy. At higher incident electron energies, the photon intensity decreases more rapidly with increasing angle than at lower energies, so that it is experimentally difficult to measure the target bremsstrahlung above the background at angles greater than 30° to 60° , even at 1.7 MeV. However, at each energy adequate measurements were obtained to allow an accurate integration of the cross section over solid angle.

Discussions of the experimental procedure, the reduction of the pulse-height distributions to cross sections, the experimental errors, and the experimental results are given below. Comparisons of the present experimental cross sections for each target material, incident electron energy, and angle are made to the Born-approximation theory and to the experiments of Motz and of Starfelt and Koch.

EXPERIMENTAL PROCEDURE

The monoenergetic electron beam from a 3-MeV Van de Graaff was used to bombard the target, which was placed in the center of a cylindrical aluminum scattering chamber. The bremsstrahlung produced in the target material and emitted at a given angle θ with respect to the incoming beam direction passed to a scintillation spectrometer through a 5-mil Mylar window in the chamber wall and then through two $\frac{1}{2}$ -in. diam, 3-in.-long lead collimators. One of these collimators was incorporated into the lead shield surrounding the spectrometer, thereby serving as the defining aperture, which subtended a geometric solid angle of 1.31×10^{-4} sr with its front surface at a distance of 98.1

* Work supported by the National Aeronautics and Space Administration.

¹ H. W. Koch and J. W. Motz, *Rev. Mod. Phys.* **31**, 920 (1959).

² J. W. Motz, *Phys. Rev.* **100**, 1560 (1955).

³ N. Starfelt and H. W. Koch, *Phys. Rev.* **102**, 1598 (1956).

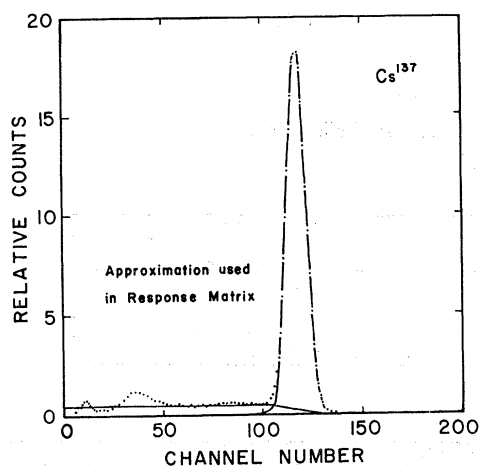


FIG. 1. Response of the bremsstrahlung spectrometer to γ rays from a Cs^{137} source. A significant reduction in the response at pulse heights less than the full-energy-absorption peak was achieved with an anticoincidence dual-crystal arrangement. This curve is typical of the response of the spectrometer at all energies up to 2.75 MeV. The simplicity of this response allowed the response matrix for the spectrometer to be determined accurately from the responses to γ rays from sources in the energy range of the present measurements.

cm from the target. A permanent magnet was placed behind the first collimator to sweep out electrons scattered in the direction of the detector. A second permanent magnet was positioned inside the chamber to deflect the electron beam downward into a carbon beam stop after it penetrated the target, in order to allow extreme forward angle detection of the bremsstrahlung without the accompanying electron beam.

The fringe magnetic field in the vicinity of the target was sufficiently weak to introduce no significant error in the determination of the incident beam direction. Beam alignment and focusing were achieved through the use of zinc sulfide viewers placed in the beam path at various points, including the target position. The 0° position for the spectrometer was determined by mapping the bremsstrahlung yield in the forward direction. Electron current on target was collected by the chamber and integrated with a standard current integrator.

Energy calibration of the electron beam was through observation of elastically scattered electrons from the thin target foils. Reference to the 625-keV internal conversion electron line from a Cs^{137} source and the 482- and 970-keV lines from a Bi^{207} source provided the energy calibration of the solid state detector used to observe the scattered electrons.

The bremsstrahlung detector was a NaI(Tl) anticoincidence spectrometer of the type used by Trail and Raboy.⁴ The response of this detector to monoenergetic γ rays is shown by the typical pulse-height distribution of Fig. 1. γ rays from calibrated sources

were used to determine experimentally the combined crystal efficiency-effective solid-angle factor of the spectrometer. The sources were placed at the target position of the chamber so that the calibration geometry was the same as that used during bombardment of the target. Sources used as standards with their respective γ -ray energies are Hg^{208} (0.279 MeV), Na^{22} (0.511 and 1.277 MeV), Y^{88} (0.899 and 1.839 MeV), and Na^{24} (2.754 MeV). Calibration precision of the sources was $\pm 5\%$ and uncertainties due to transition branching and internal conversion were negligible. The estimated accuracy of the combined efficiency-effective solid-angle determination after several independent measurements is $\pm 3\%$ in the photon-energy range $k < 2.0$ MeV and $\pm 5\%$ for $k > 2.0$ MeV.

Self-supporting targets of Al, Cu, Sn, and Au, prepared by vacuum evaporation, were sufficiently thin to reduce multiple scattering to a negligible level. To assure that the targets were thin enough, bremsstrahlung measurements were made on more than one thickness for each material. Typical thicknesses of the targets used in these measurements were: Al, $795 \mu\text{g}/\text{cm}^2$; Cu, $1040 \mu\text{g}/\text{cm}^2$; Sn, $485 \mu\text{g}/\text{cm}^2$; and Au, $398 \mu\text{g}/\text{cm}^2$.

Since the number of counts in a typical pulse-height spectrum ranged over two or three orders of magnitude downward from low photon energy to the high-energy end, a second run was made in each case using a lead "beam hardener" inserted between the target and the detector to reduce the high count rate substantially at low photon energies while reducing the rate in the region $k > 0.7 T_0$ by less than 15%. This technique improved the statistical accuracy near the spectral end points without introducing pulse pile-up effects due to increasing the already high count rate at low photon energies. Each spectrum, therefore, is comprised of a spectrum taken without the hardener, joined at approximately $0.7T_0$ to the spectrum from the hardener run corrected for photon attenuation in the hardener material.

Background effects were removed from the pulse-height distributions by inserting a tantalum photon absorber between the target and the detector with the target in place and subtracting the resulting spectrum from that taken without the absorber. The geometry of the absorber was chosen so as to shield only the target from the detector, leaving exposed the background-producing surfaces. The thickness of the tantalum absorber was 3.97 cm. Calculated photon transmission at 2.5 MeV, the highest energy for which measurements were made, was less than 7%. Spectral distortion due to background subtraction in this manner was experimentally investigated during measurements of bremsstrahlung production in thick targets. During bombardment of thick targets of low- Z material, negligible background is produced since the electrons are stopped in the targets. Total transmission of the absorber material in this case for all photon energies was observed to be less than 1.5%. Spectral distortion was

⁴ C. C. Trail and Sol Raboy, Rev. Sci. Instr. 30, 425 (1959).

found to be less than 1% below 1.5 MeV photon energy, approximately 2% for $1.5 < k < 2.2$ MeV, and 5% for $k > 2.2$ MeV.

DATA REDUCTION

Various methods of spectrometer response removal from the pulse-height spectra were attempted. The difficulty encountered in applying such techniques as response matrix inversion or iterative procedures is that oscillations are produced in the spectra due to statistical fluctuations in the input spectra. The matrix-inversion technique involves the additional difficulty of accurately carrying out the inversion process itself. Oscillations can be avoided, however, by operating on smooth data derived from the pulse-height data. To determine the cross-section values presented here a variation of an iterative method was applied in which the input spectra were hand-smoothed pulse-height distributions. The smoothed spectra were multiplied by the detector response matrix, thus yielding a "smeared" spectrum to simulate the effects of measurement. A set of correction factors was derived by taking the ratio of the smoothed spectrum to the "smeared" spectrum. The original unsmoothed pulse-height distributions were multiplied by these ratios to obtain corrected spectra. This method of response removal was shown by use of test spectra to be accurate to within a few percent in the photon energy region below $k = 0.9T_0$. In the region $k > 0.95T_0$, however, where large corrections were necessary, this method tended to undercorrect the pulse-height spectra by about 15% on the average. The greatest inaccuracy occurred where the spectral cutoff was sharp, such as for the Sn and Au data. Rather than applying further iterations to remove this deficiency, it was considered sufficiently accurate to simply apply an additional 15% correction in this region. With the undercorrections taken into account, there is still added uncertainty in the cross sections in the region $k > 0.9T_0$ reported here due to the response removal, since the corrections near the end point depend strongly on the detailed shape of the pulse-height distribution in the pulse-height region corresponding to $k > 0.75T_0$. Where many spectra are to be analyzed, as in the present case, it is impracticable to find the correction factors for each case because of the necessity for hand-smoothing the pulse-height spectra. The present analysis consisted of finding the correction factors for classes of pulse-height distribution shapes. Pulse-height distributions in the various shape categories were then corrected by the appropriate set of factors for their class. Thus this procedure did not allow for the small differences within the shape classes.

The spectra corrected for the spectrometer response were then corrected for the spectrometer efficiency. Examples of the combined corrections applied to the pulse-height data are given in Fig. 2. Shown are correction factors for Au at $\theta = 0^\circ$ and $T_0 = 1$ MeV and for Al at $\theta = 0^\circ$ and $T_0 = 1$ MeV. The Au correction

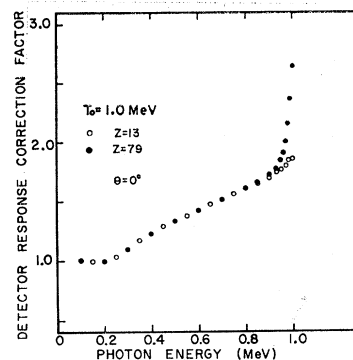


FIG. 2. Correction factors for the removal of spectrometer response from the pulse-height distributions.

ratios are typical of the corrections made to most of the spectra. The Al correction factors differ from those of Au near the end point. This difference arises from the difference in the spectral shapes at the end point. Most of the spectra fall off sharply at the high-energy end, while at the forward angles 0° and 4° , the Al and Cu spectra drop off smoothly in magnitude with considerably less curvature near the end point.

EXPERIMENTAL ERRORS

The accuracy of the experimental cross-section values is limited by two types of errors. The first type causes a shift in the entire spectrum from the true value, and has a constant magnitude for each incident energy and photon angle. The second type can both shift the spectrum and distort its shape. The magnitude of the error may also vary with incident energy and photon angle.

For the present results, estimates of the limits of the errors falling in the first category are

- (1) Target current: $\pm 2\%$.
- (2) Target thickness and uniformity: $\pm 5\%$.

Estimates of the chief experimental errors in the second category, in addition to those discussed in the previous section are

(1) Photon angle: $\pm 0.3^\circ$. This uncertainty in angle produces the greatest error in the spectra for $10^\circ < \theta < 60^\circ$ because of the strong dependence of the yield on angle in this region. Furthermore, this angular dependence and the resulting error increases with increasing electron incident energy. A maximum uncertainty of 6% in the 1.0-MeV values and 12% in the 2.5-MeV values is estimated.

(2) Statistical errors. The statistical fluctuation is in every case most pronounced near the spectral end point, because the count rate is several orders of magnitude below that at low photon energies. The statistical accuracy of data near the end point is limited by the rate at which data can be accumulated without pulse pile-up effects, as compared to the count rate of the room

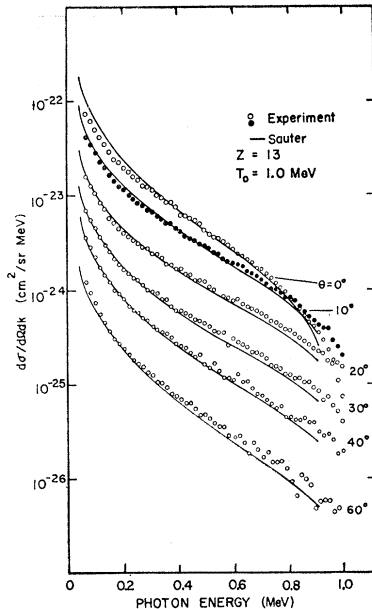


FIG. 3. Cross sections differential in photon energy and solid angle for production of bremsstrahlung by 1.0-MeV electrons incident on an Al target. Comparison with the Born-approximation theory, shown as solid lines, is not meaningful in the region near the end points since this theory is not valid in this region. However, at lower photon energies, the experiment and theory are in reasonable agreement.

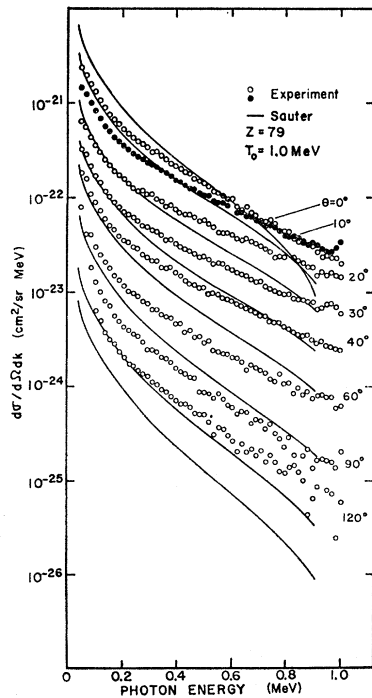


FIG. 4. Differential cross sections for production of bremsstrahlung by 1.0-MeV electrons incident on a Au target.

background. The photon energy interval for which the statistical uncertainty is appreciable becomes greater with increasing angle. At 0° and 4° the error is less than 4% below $0.8T_0$, while at the largest angle the statistical error is estimated to be less than 8% below $0.5T_0$, increasing to approximately 30% at $0.9T_0$.

(3) Spectrometer response removal. The error introduced into the spectra from this correction is less than 3% for $k < 0.9T_0$. In the region $k > 0.9T_0$ the error increases to a maximum of 30–50% at the end-point value.

EXPERIMENTAL RESULTS

The present experimental results for an incident electron energy of 1.0 MeV at $\theta = 0^\circ, 10^\circ, 20^\circ, 30^\circ, 40^\circ,$ and 60° for an Al target are shown in Fig. 3. Similar

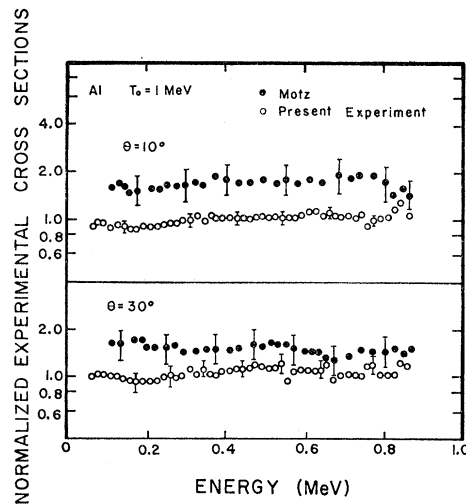


FIG. 5. Comparison of present cross-section values with the results of Motz (Ref. 2) at 1.0 MeV for Al. Both sets of data are normalized to the Born-approximation theory.

data for Au are shown in Fig. 4, except that additional angles of 90° and 120° are included. For the Al target the present measurement indicates reasonably good agreement with the Born-approximation theory except near the end point, where it is expected that the theory would least apply. There is a tendency for the experimental values to be somewhat less than the theoretical values at the small angles ($0^\circ, 4^\circ,$ and 10°) in the photon energy region $k < 0.4T_0$, due to screening of the nucleus by the atomic electrons. The reduction in yield in the low-energy region of the spectrum increases for the Au target. For Au at 0° the experimental value is 30% below the theory at $k = 0.2$ MeV and crosses the theory at $k = 0.6$ MeV. At 20° and larger angles the experiment is equal to or greater than the theory at all photon energies for Au. This trend is also observed by Motz for the Au target. The comparison of the present data to that of Motz for Al at 10° and 30° is given in Fig. 5. A comparison of the two experiments

for Au at 0°, 20°, 30°, and 90° is shown in Fig. 6. The data are normalized to the Born-approximation values. It is readily seen that a disagreement outside the limits of errors between the two experiments exists for the measurements on both Al and Au targets. The largest differences appear to occur in the photon energy region below $k=0.7T_0$. At higher photon energies the two measurements become closer, merging near the high-frequency limit of the spectra.

The measurements at 1.0 MeV on targets of Cu and Sn are shown in Figs. 7 and 8. For the purpose of clarity the data at 4° for all the targets are plotted in Fig. 9 as a separate figure, since they overlap values at 0°

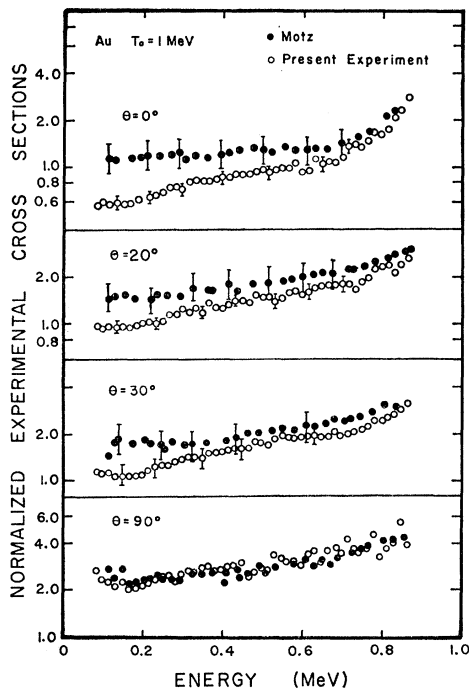


FIG. 6. Comparison of present cross-section values with the results of Motz at 1.0 MeV for Au. As in Fig. 5, the data have been normalized to the Born-approximation theory.

and 10°, which cross near the end point. An increasing enhancement of the photon yields with atomic number is observed near the end points of the spectra. The effect of screening is also observed to become more significant with increasing atomic number.

At 1.7 MeV the cross sections measured from Al targets are in quite good agreement with the Born-approximation values out to a photon energy of 1.4 MeV, as seen in Fig. 10. The effect of screening can be observed in the spectra at 0°, 4°, and 10°, where the measured values, as at 1.0 MeV, fall 10% or so below the theory for photon energies $k < 0.3$ MeV. The Cu data at 1.7 MeV, shown in Fig. 11, indicate that the discrepancy between the experiment and theory has decreased as compared to 1.0 MeV, although generally

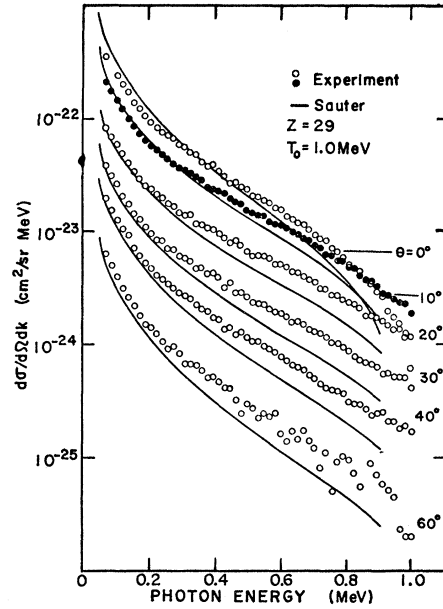


FIG. 7. Differential cross sections for production of bremsstrahlung by 1.0-MeV electrons incident on a Cu target.

the data are still above the theory. Likewise for Sn and Au, the experimental cross sections, shown in Figs. 12 and 13, are closer to the Born-approximation values. The trend with angle for each target appears to be the same as the trend at 1.0 MeV.

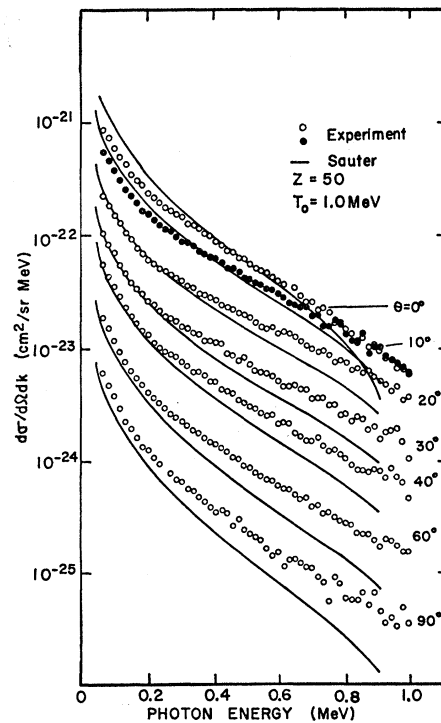


FIG. 8. Differential cross sections for production of bremsstrahlung by 1.0-MeV electrons incident on a Sn target.

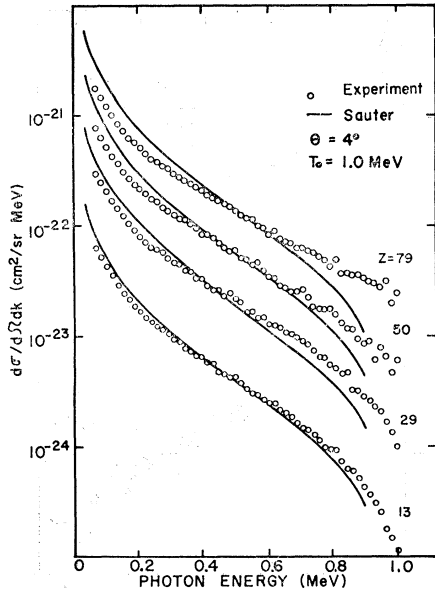


FIG. 9. Differential cross sections at 4° for production of bremsstrahlung by 1.0-MeV electrons incident on Al, Cu, Sn, and Au targets.

At 2.5 MeV and angles of 4° , 10° , and 20° in Fig. 14, the experimental cross sections for Al and the theory are in excellent agreement except in the region near the end point. However, at 0° the experimental values fall below the theory out to about $k=1.8$ MeV. A

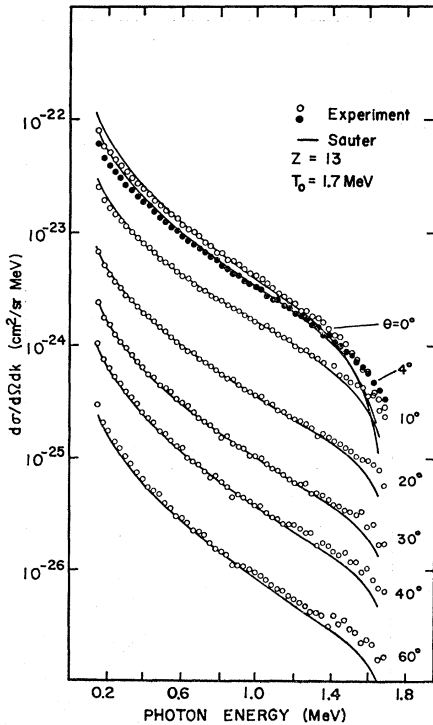


FIG. 10. Differential cross sections for production of bremsstrahlung by 1.7-MeV electrons incident on an Al target. Little change is observed for Al at 1.7 MeV as compared to 1.0 MeV.

comparison of the present measurement on Al at 2.5 MeV and 0° with the measurement of Starfelt and Koch³ at 2.72 MeV is made in Fig. 15. Both data are presented, normalized to the Born-approximation values. The abscissa is the ratio of the photon energy to the incident electron energy. The agreement between the two experiments appears to be good up to about $k=0.7T_0$, where considerable scatter begins, largely due to the statistics of the points near the end of the spectrum of the data of Starfelt and Koch. For both experiments the uncertainty at the end point becomes large because of reduced statistical accuracy. Also, in this region the greatest corrections for spectrometer response

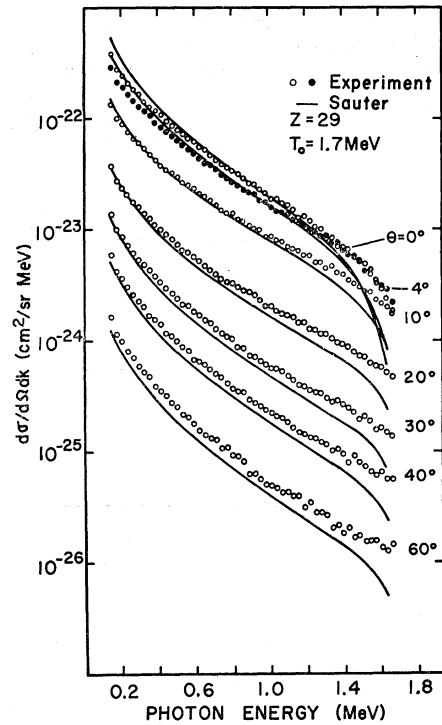


FIG. 11. Differential cross sections for production of bremsstrahlung by 1.7-MeV electrons incident on a Cu target. At 1.7 MeV the experimental data appear to lie closer to the Born-approximation theory than at 1.0 MeV.

are applied, which introduce additional uncertainties. The results for Au at 2.5 MeV are shown in Fig. 16. At 20° and 30° , the largest angles for which accurate data could be obtained at this energy, the experimental values are closer to the theory than at 1.7 MeV. However, the spectra are still harder than those predicted by the theory. The experimental cross sections at 0° for Au are well below the theory, as at 1.7 MeV. A comparison of the two experimental results for Au is shown in Fig. 15. The two experiments are in good agreement.

The measurements on Cu and Sn targets are shown in Figs. 17 and 18. The cross-section values measured for Cu, except near the spectral end points, are close to

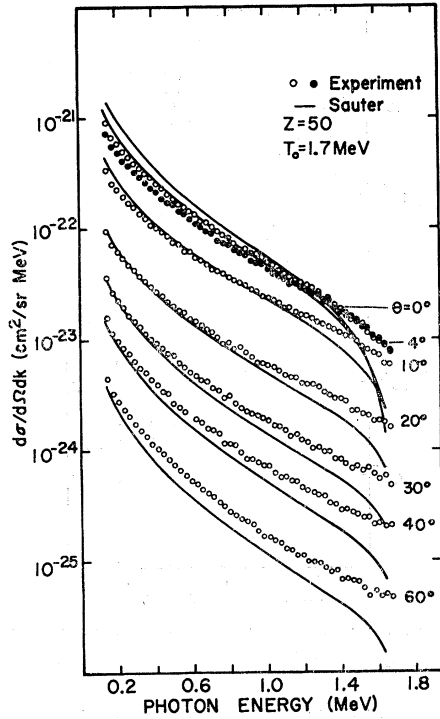


FIG. 12. Differential cross sections for production of bremsstrahlung by 1.7-MeV electrons incident on a Sn target. As was the case for Cu, the 1.7-MeV cross sections measured for Sn are closer to the theory at 1.7 MeV than at 1.0 MeV.

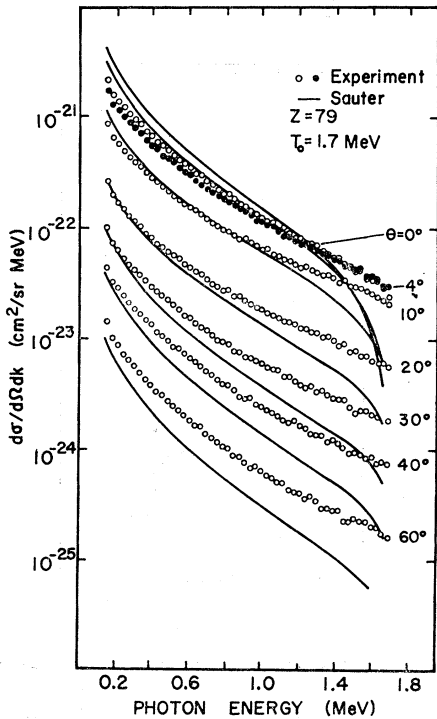


FIG. 13. Differential cross sections for the production of bremsstrahlung by 1.7-MeV electrons incident on a Au target.

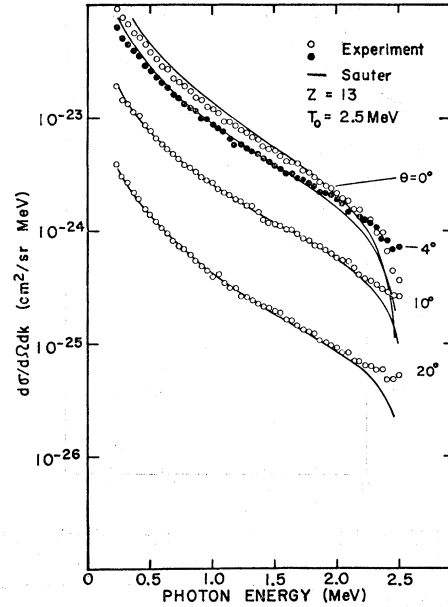


FIG. 14. Differential cross sections for the production of bremsstrahlung by 2.5-MeV electrons incident on an Al target. At 0° the experimental values are below the theory for $k < 1.8$ MeV.

the theoretical predictions at angles other than 0°, where experimental values are below the theory, and at 30°, where the experimental values are somewhat above the theory. The measured cross-section values for Sn are also generally close to the theory except for the small-angle values and at the end points.

Cross sections, differential in energy only, obtained

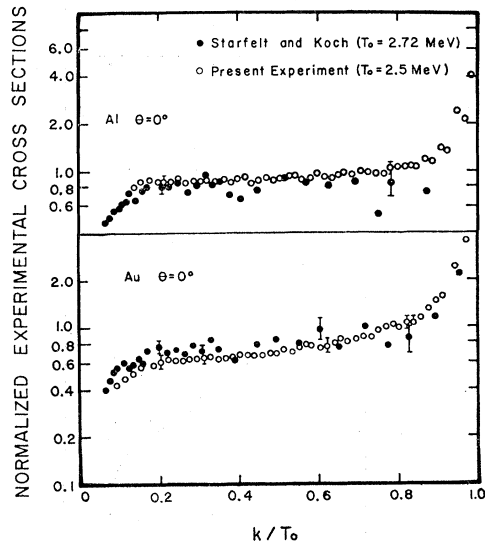


FIG. 15. Comparison of the present 0° experimental results for Al and Au at 2.5 MeV with those of Starfelt and Koch (Ref. 3) at 2.72 MeV. The abscissa is the ratio of the photon energy to the incident electron energy. The experimental values are normalized to the Born-approximation theory. The two experiments are in agreement within the quoted experimental errors.

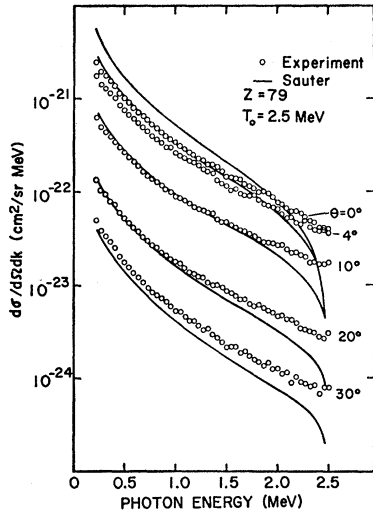


FIG. 16. Differential cross sections for the production of bremsstrahlung by 2.5-MeV electrons incident on a Au target. At this energy the experimental values are closer to the theory than at 1.0 and 1.7 MeV.

by integrating the preceding cross sections over solid angle are shown in Figs. 19–21. As was done for the previous results, the experimental values are plotted with the Born-approximation theory for comparison. A shift of the experimental results with energy, relative to the theory, is observed for Sn and Au. The results for Al and Cu, relative to the theory, appear to be nearly constant with energy. Estimates of the high-frequency limit of the cross sections for Al and Au are indicated in the figures. The estimates were taken from Koch and Motz.¹ They were derived by U. Fano⁵ and corrected by Fano, Koch, and Motz.⁶ The corrected

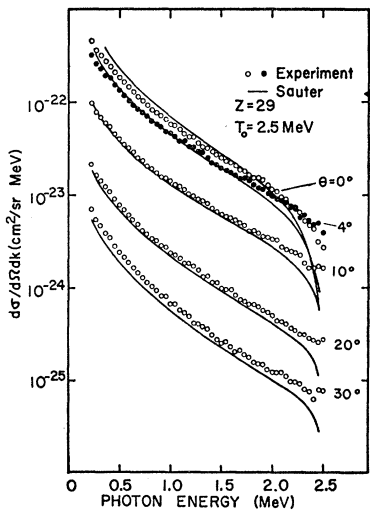


FIG. 17. Differential cross sections for the production of bremsstrahlung by 2.5-MeV electrons incident on a Cu target.

⁵ U. Fano, Phys. Rev. **116**, 1156 (1959).

⁶ U. Fano, H. W. Koch, and J. W. Motz, Phys. Rev. **112**, 1679 (1958).

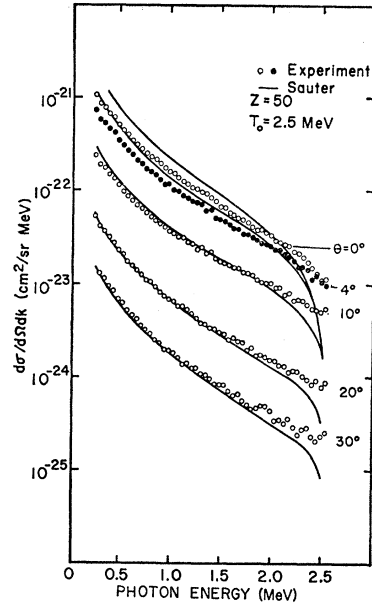


FIG. 18. Differential cross sections for the production of bremsstrahlung by 2.5-MeV electrons incident on a Sn target.

cross-section values for Au accurately predict the experimental cross-section values at the end point. For Al the comparison is not as good. However, the end-point determination for Au can be made more accurately than for Al because of the significant enhancement of the high-energy end of the photon spectrum for the higher atomic number.

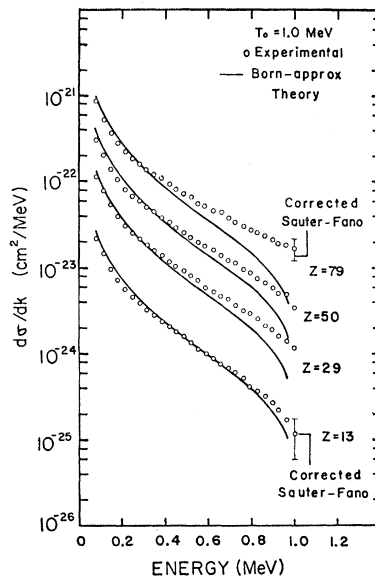


FIG. 19. Cross sections differential in photon energy at $T_0 = 1.0$ MeV, resulting from integration of the previously presented data over solid angle. The experimental values are compared to the Born-approximation cross sections. For Al and Au the corrected Sauter-Fano (Ref. 6) values at the high-frequency limit are indicated.

CONCLUSIONS

The disagreements between the measurements of Motz² at 1.0 MeV for Al and Au and the present measurements are well outside the quoted experimental errors. Except for background removal and detector shielding and collimation, the two experiments are similar. In obtaining the present results, background spectra were obtained with the target foil in place, as described in the section on experimental procedure. This method allowed the background resulting from the beam which had passed through the target to be removed from the total spectra. Such a procedure is desirable since the scattered-beam distribution which produces thick-target bremsstrahlung in the chamber is the same during the background accumulation as it was during the accumulation of the target bremsstrahlung. In the experiment of Motz, however, background spectra were obtained with the target removed. Present background intensities for Al at 1.0 MeV and 0° amounted to 14% of the total spectra, with spectral

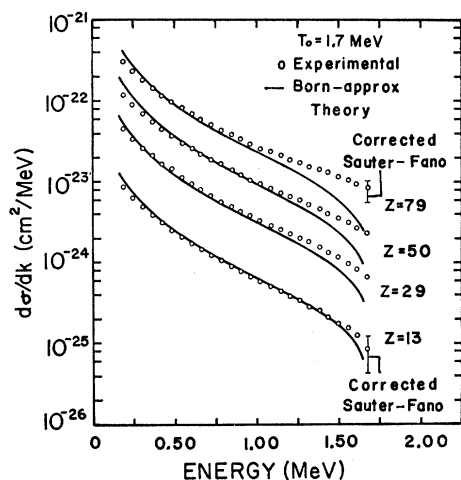


FIG. 20. Cross sections differential in photon energy at $T_0=1.7$ MeV resulting from integration of the data over solid angle.

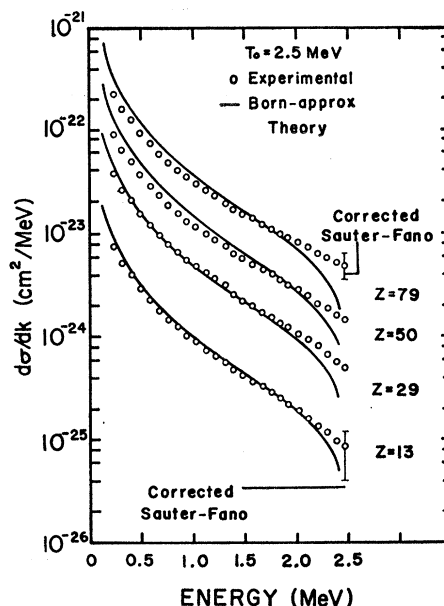


FIG. 21. Cross sections differential in photon energy at $T_0=2.5$ MeV.

distributions characteristic of those from thick targets, i.e., falling off more rapidly at the high-energy end of the spectrum. Backgrounds observed by removing the targets amounted to only 2% of the total spectrum. An example background reported by Motz was about 10% of the net spectrum. The magnitude of the relative backgrounds with target in (and blanked to the detector) and target out depends strongly on the shielding afforded the detector, and the detector collimation. The agreement with Starfelt and Koch at higher energy substantially reinforces the present measurements at lower energy. The same targets and experimental techniques were used in all the reported measurements. In view of the conflicting experiments at 1.0 MeV and the present interest in the electron-bremsstrahlung process, it would be desirable to extend the measurements to lower incident electron energies.